MULTISCALE MODELING OF THE LOW-TEMPERATURE ELECTRON IRRADIATION OF BERYLLIUM

M.I. Bratchenko, S.V. Dyuldya
National Science Center "Kharkov Institute of Physics and Technology", Kharkov, Ukraine
E-mail: sdul@kipt.kharkov.ua

Presented are the methodology and the results of the multiscale modeling of radiation defects primary production and time evolution for 2.5 MeV cryogenic (77 K) irradiation of highly deformed to ~ 10^{12} cm^{-2} dislocations density beryllium at the NSC KIPT electron linac ELIAS. It is shown that the application of low-temperature e^--irradiation of prestrained targets allows efficient suppression of vacancy-interstitial recombination due to escape of freely migrating self-interstitial atoms to dislocation sinks and results in abnormally high (~ 10^{-3} per atom) vacancy yield comparable with that of primarily produced Frenkel pairs at a reasonable (≤ 10^3 h) e^--beam exposure.

PACS: 61.80.-x, 61.82.Bg, 61.72.Cc, 61.80.Fe, 07.05.Tp, 02.70.Ns, 02.70.Uu

1. INTRODUCTION

The NSC KIPT sited charged particles accelerators are widely used to support R&D of radiation damage (RD) physics and radiation material science (RMS). Major applications of the ion beam (IB) machines concern the *'simulation irradiation'* (SI) concept targeted on the prediction of reactor (n, γ) irradiation induced effects in materials. The required IB exposure of SI experiments is planned on the basis of calculation of the primary RD (PRD) dose measured in the number of atomic displacements per atom, N_{dpa}. The established standard practice [1] considers dpa only as *"a unit of radiation exposure"*: N_{dpa} shall be calculated coherently for both the targeting reactor and the accelerator irradiation environments in a strict accordance with the Norgett-Robinson-Torrens proposed *'NRT standard'* model [2]

$$N_{\text{dpa}}^{(\text{NRT})}\left(E_{\text{PKA}}\right)=\kappa\cdot E_{\text{D}}\left(E_{\text{PKA}}\right)/2E_{\text{d}} \qquad (1)$$

which is a generalization of the famous Kinchin-Pease model primarily developed to estimate the number of point defects in an atomic collision cascade (ACC) initiated by the primary knock-on atom (PKA) of a given energy E_{PKA}. Here $\kappa = 0.8$, $E_{\text{D}}(E_{\text{PKA}})$ is the *"damage energy"*, the total elastic energy loss of a PKA available to produce displacements, and $E_{\text{d}} \sim 10^1 \ldots 10^2$ eV is the material-specific displacement threshold energy.

The validity of the NRT standard is confined in the area of comparative dosimetry of reactor/accelerator based neutron/ion damage of metals and alloys [3]. The number of NRT dpa cannot be directly measured experimentally and thus does not represent an observable physical quantity. Instead, one must consider the actual RD metrics, the atomic concentrations C_{FP} of Frenkel pairs (FPs) as well of their constituents, C_{V} of vacancies (V) and C_{I} of self-interstitial atoms (SIAs).

The observable $C_{\text{V,I}}$ are orders of magnitude smaller than the NRT calculated dpa because of several reasons [4, 5]. First, FPs annihilate inside the 'hot' ACC core during its athermal quenching stage, ~ $10^{-(13\ldots11)}$ s. This is essential [4] for fast neutron and ion impact when successive atomic displacements occur at a distance ~ a, the lattice constant of a material. But it is not so topical for the moderate (~ MeV) energy electron beams (EBs) impact when only isolated spatially separated FPs appear. Next, the PRD stage produced defects evolve in space and time through the complex short-term (~ $10^{-(11\ldots6)}$ s) kinetic stage of their recovery and agglomeration into complexes till the thermal diffusion stage (> 10^{-6} s) of their recombination and interaction with sinks. Finally, this is asymptotically forming the saturated damaged state of a material which results in the observed irradiation induced changes of macroscopic properties.

The complexity of the self-consistent description of the whole RD picture (which covers 13…20 orders of magnitude of temporal development at a spatial scale $10^{-8}\ldots10^2$ cm) gave birth to the novel Multiscale Modeling & Simulation (MSMS) paradigm of the RMS computer modeling studies [6]. It involves the problem-specific sequence of diverse methods and input/output data concordant codes: *ab initio* quantum mechanics (QM), classical Molecular Dynamics (MD), kinetic Monte-Carlo (kMC) and reaction rate theory [5, 7] calculations, dislocation dynamics [7], and Finite Element Method (FEM). Each of them simulates its own scale of the spatiotemporal evolution to transfer outputs to the subsequent scale. Recently we have proposed [8] the MSMS program incorporation into the computational support of the NSC KIPT accelerator based irradiations and identified the appropriate simulation software toolbox [9].

The present paper encompasses the results of our first attempt to push the rationale and planning of NSC KIPT irradiations of materials *'beyond NRT'*. We present the results of the trans-NRT MSMS of the accumulation and evolution of point defects in a highly deformed high-purity hcp Beryllium, a structurally complex anisotropic functional material, for the case of its cryogenic irradiation at the NSC KIPT EB linac ELIAS.

2. PROBLEM STATEMENT

Beryllium manifests the non-trivial properties and effects (*e.g.*, superplasticity) promoted by its pronounced anisotropy [10, 11]. This also applies to Be low-temperature physics regarding its electronic structure and transport properties, and particularly the structural sensitivity of its superconducting transition temperature T_{c}.

Without going into details that go beyond the scope of this paper, let's declare that the experimental investigation of this lattice defects density-of-state dependent effect requires high concentrations of the cryogenically

'frozen' vacancies, $C_V \sim 10^{-3}$ per Be atom [12], much greater than the thermal equilibrium C_V. The extra non-equilibrium vacancies can be injected by e^--irradiation. However, the elastic displacement cross-section σ_d [13] based calculation shows that even the most conservative estimate of C_V as the concentration of as-irradiated primary FPs yields $C_{FP} \sim 10^{-(5\ldots4)}$ per atom per day of exposure to ~ MeV energy EB. The thermal diffusion activated recombination V + I = ∅ does diminish C_{FP} by orders of magnitude. So, the problem looks insoluble.

Nevertheless, it has been put forward [14] an idea to solve it by means of the V–I recombination suppression with the following experimental setup: (i) to apply the nitrogen temperature $T = 77$ K e^--irradiation when only SIA are diffusively mobile; (ii) to use the high-purity Be target which is beforehand highly deformed up to the dislocation densities $\rho_d \sim 10^{11\ldots12}$ cm^{-2} granting the highest possible concentration of SIA sinks, and (iii) to transfer the unheated irradiated sample into the helium temperature appliance for subsequent measurements.

Despite of the extreme conditioning of each step of this scenario, it is in fact feasible by means of the NSC KIPT developed processes of high-purity Be samples preparation and cryogenic e^--irradiation at the accelerator ELIAS. It is worth noting the NSC KIPT ELIAS team advanced capability to provide immediate post-irradiation examination of samples (without their warming-up) at the same (or lower) temperature.

The goal of the present work is the computational substantiation of the proposed technique by means of the MSMS calculation of the utmost value of C_V obtainable at the ELIAS e^--irradiation. For this purpose, we apply the subset of our MSMS software toolkit [9] embracing (i) the in-house developed GEANT4 Toolkit based radiation transport (RT) Monte-Carlo (MC) code RaT 3.1 [15], (ii) the LAMMPS MD [16], and (iii) the SPPARKS kMC [17] packages developed and freely distributed by the U.S. Sandia Nat. Lab. team.

3. PRIMARY RADIATION DAMAGE

Without loss of generality, we consider a semi-infinite planar target of $\rho_{Be} = 1.85$ gm/cm^3 dense polycrystalline beryllium irradiated by a broad parallel e^--beam with the nominal parameters of the ELIAS linac: the EB energy $E_e = 2.5$ MeV, the current density $j = 10$ μA/cm^2, the e^--flux $\phi = j/e = 6.24 \cdot 10^{13}$ $e^- \cdot$cm$^{-2} \cdot$s^{-1}.

An adequate computer modeling of the shortest-time ballistic stage of the as-irradiated PRD was conducted by means of the RaT 3.1 MC code using the GEANT4.9.5 supplied algorithms and data for simulation of energy losses and multiple scattering of relativistic electrons in matter. Relatively rare events of the strong electron–atom displacing collisions were sampled according to the Mott elastic scattering [13] cross-section σ_d calculated for the NRT standard recommended value of the displacement threshold energy $E_d = 31$ eV of beryllium.

Trajectories of electrons and γ-quanta of the radiation cascade as well as those of all Be recoils (both PKAs and secondary knock-ons, SKAs, of the ACC) were traced until a 'thermalization' i. e. down to the energy E_{min}, ~ 100 eV for e^-, and ~ 1 eV for cascade atoms. Due to fairly short ranges, E_{min} are small enough to not affect the calculated spatial distributions *vs.* the EB penetration depth z. Note that the ACC was modeled explicitly i. e. using the RaT code specific algorithm and data [15, 3] validated against those of the SRIM package, a practical standard of the IB induced PRD evaluation.

Primary results of simulation concerning the EB penetration into a target are presented in Fig. 1. The depth profile of thermalized electrons spreads up to the EB extrapolated projected range $R_p \approx 1$ cm. Only the bremsstrahlung produced secondary Compton electrons are present at $z > R_p$. At $z < R_p$, the profile is drawn (roughly exponentially) until a broad maximum, at $z \approx ¾R_p$, which is due to the complex interplay of energy loss, straggling, and multiple scattering of electrons.

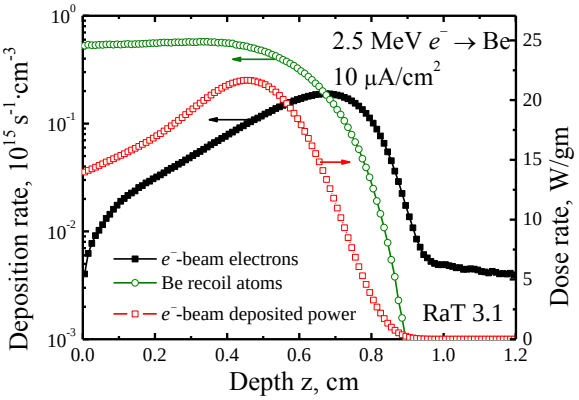

Fig. 1. The Monte-Carlo calculated depth profiles of the EB specific power deposition (□) and thermalized particles, electrons (■) and Be recoil atoms (○)

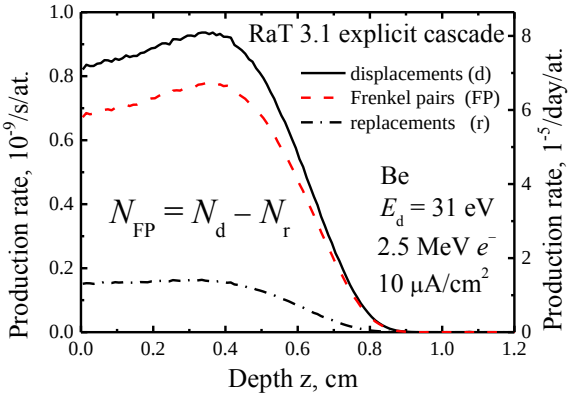

Fig. 2. The atomic displacement (dpa) rate depth profile subdivided into contributions of the actually formed Frenkel pairs and the Be–Be atoms replacements

We supplemented Fig. 1 with the standard dose (or the mass specific power deposition) rate profile $P_{dep}(z)$. In itself, the EB deposited power does not affect the RD of metal targets [4, 5]. But it is essential for the maintenance of the thermal regimes of cryogenic e^--irradiation. Note that P_{dep} is high as compared with the γ-heating relevant ~ 0.1…1 W/gm of in-pile test channels. The $P_{dep}(z)$ maximum is shifted to lower $z \approx ½R_p$ where electrons are energetic enough to heat the target and to displace the lattice atoms. Be recoils (both subthreshold ones, and PKAs) are distributed almost uniformly right up to this depth, as shown in greater details in Fig. 2.

The maximal atomic displacement rate occurs at the depth $z = 4$ mm $\approx 0.4 \cdot R_p$ and exceeds the target surface ($z = 0$) value only by ≈ 14%. But only ≈ 80% of displacements ($E_{PKA} > E_d$) are actual FPs. The rest ≈ 20% of them do not form a point defect but result in

the replacement of one Be atom with another. They are due to the $E_d < E_{PKA} < 2 \cdot E_d$ range of the PKA energy spectrum.

The explicit modeling of an ACC and the simplified NRT standard approach (1) treat the partitioning of displacements onto FPs and replacements somewhat differently [3]. This results in the systematic bias of the actual $N_{FP} = N_I \equiv N_V$ and $N_{FP}^{(NRT)} \equiv N_{dpa}^{(NRT)}$ shown in Fig. 3. One can see that the NRT standard always underestimates the number of actually produced point defects.

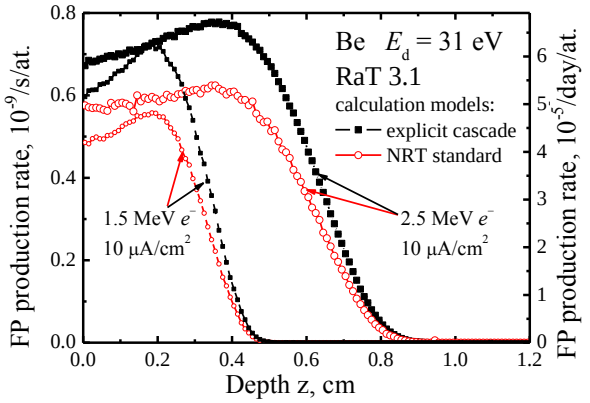

Fig. 3. The FP depth profiles of Be PRD by EB of different energies MC calculated in the NRT standard approximation (○) and by the explicit ACC modeling (■)

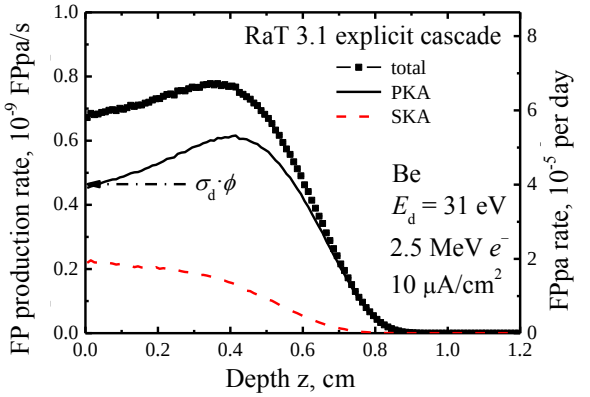

Fig. 4. The Be target PRD depth profile (■) partitioned into contributions of primary (solid curve) and secondary cascade (dashed curve) knock-on atoms

The ratio $\chi = N_{FP} / N_{FP}^{(NRT)} > 1$ is only weakly depth dependent in the highly damaged area ($z < ½R_p$) of a target; $\chi = 1.2 \ldots 1.25$ for both 1.5 MeV and 2.5 MeV e^--irradiations of Be. But χ is known to grow with energy (and mass) of a projectile when the PKA spectra become harder, the secondary displacement function (SDF) increases, and ACCs become more and more developed. For the LPE-10 linac 10 MeV e^--irradiation of Ni–Cr alloy 690, $\chi \approx 1.5$, and amounts $\chi \approx 2$ for heavy ions irradiation of structural steels [3]. This is significant enough to opt for the explicit cascade modeling for estimations of the actual concentrations of the V–I Frenkel pairs.

For not to get it mixed up with the conventional NRT dpa, it is expedient to introduce the special unit of measurement, FPpa = χ×(NRT dpa). We shall use it below for the topical case of the current study.

In Fig. 4, the dash-dotted arrow indicates the FPpa rate calculated analytically using the total displacement cross-section [13] $\sigma_d(E_e, E_d) = 7.44$ barn for the initial EB energy. It is fairly consistent with the zero-depth extrapolation of the MC simulation data for the contribution of PKAs immediately displaced by electrons. However, it covers only two thirds (≈ 66%) of the actually modeled total FPpa rate (markers) in a thin target. The remaining one third is due to the ACC development.

The atomic collision cascades are frequently ignored in a planning of the EB PRD production. Sporadic ACCs are considered irrelevant to the electron impact and a simple formula $C_{FP} = \sigma_d(E_e, E_d) \cdot \phi \cdot t_0$ is applied for the EB exposure duration t_0. The Fig. 4 data show the drawbacks and quantitative limitations of this approximation namely for the case of thin targets. The exact MC modeling is favorable to obtain the reliable data.

For the subsequent MSMS calculations, we adopt, from Fig. 4, the conservative zero-depth estimate of the PRD FP production rate $K_0 = 7 \cdot 10^{-10}$ FPpa/s.

4. THE REACTIONS RATE THEORY ANSATZ AND MODEL ESTIMATES

The $C_{V,I}(\mathbf{r},t)$ spatiotemporal evolution at the next timescale of the RD development and subject to (V,SIA) thermal diffusion and reactions with each other and with sinks is generally described by the partial derivative master equations of the RD rate theory [7]. For the limited purpose of the current study, we neglect gradient terms and confine ourselves to the mean-field approximation of the reaction rate theory [5, 7] taking into account the problem specific simplifications. In this case, the time derivatives $\dot{C}_{V,I}(t)$ are governed by the following system of the ordinary differential equations (ODE)

$$\begin{cases} \dot{C}_V(t) = K(t) - \mu_R D_I \cdot C_I(t) \cdot C_V(t), & (2.1) \\ \dot{C}_I(t) = \dot{C}_V(t) - k^2 D_I \cdot C_I(t), & (2.2) \end{cases}$$

where the source term $K(t)$ is the FPpa production rate, $K(t) = K_0$ for $t \le t_0$ (EB on), $K(t) = 0$ otherwise (EB off); D_I, cm$^2 \cdot$s^{-1}, is the SIA diffusion coefficient; μ_R, cm^{-2}, is the V–I recombination constant and k^2, cm^{-2}, is the total sink strength [5] for SIAs. In Eq. 2, it is assumed that only SIAs are mobile ($D_V = 0$).

The ODE system (2) was readily solved numerically for the initial conditions $C_{V,I}(0) = 0$ (we neglect the equilibrium $C_V(0) << 10^{-6}$ for a cryogenic irradiation) and benchmarked against the asymptotic solution [5]

$$C_V(t_0) \approx \begin{cases} K_0 t_0 \equiv C_{FP}(t_0), & t_0 < t^* \quad (3.1) \\ K_0 \cdot \sqrt{t^* t_0} \equiv C_{FP}(t_0) \cdot \sqrt{t_0 / t^*}, & t_0 >> t^* \quad (3.2) \end{cases}$$

where the characteristic time $t^* = \varepsilon / K_0$ scales with the dimensionless ratio $\varepsilon = k^2 / \mu_R$ rating the sink absorption of a SIA to its recombination with a vacancy. For short $t_0 < t^*$ of ballistic PRD irradiation exposure, $C_V \propto t_0$. For $t_0 > t^*$, the diffusion limited buildup of vacancies is slowing down very notably; asymptotically, $C_V \propto \sqrt{t_0}$.

First, we estimated $C_V(t)$ by applying some synoptic RMS models and reference data for Be.

Assuming that the only SIA sinks are edge dislocations, we evaluated the dislocation sink strength k^2 according to the Nichols isotropic model [18]

$$k^2 = 2\pi\rho_d \Big/ \left(\ln \frac{R_d}{r_c} - \frac{3}{4} \right) , \quad (4)$$

where $R_d = (\pi\rho_d)^{-½}$ is the dislocation cylindrical unit cell radius and r_c is the dislocation core radius, $\sim a = 2.3$ Å for Be. This yields $k^2 \approx 10^{12}$ cm^{-2} for $\rho_d = 10^{11}$ cm^{-2}.

The recombination constant $\mu_R \approx 4\pi r_{eff}/\Omega_{Be}$ was estimated from the effective SIA capture radius r_{eff} of a vacancy and the atomic volume Ω_{Be}. Since the MD data derived $r_{eff} \approx 2a$ [7], $\mu_R \approx 10^{17}$ cm$^{-2} >> k^2$, and $\varepsilon << 1$.

The SIA self-diffusion coefficient D_I is strongly temperature T dependent

$$D_I = D_0 \cdot \exp\left(-E_m \big/ k_B T\right), \qquad (5)$$

where k_B is Boltzmann's constant and E_m is the SIA migration barrier energy. In Be, the pre-exponential factor $D_0 \approx 0.62$ cm^2/s [11] while E_m is highly anisotropic.

Vladimirov and coworkers carried out an extensive *ab initio* QM MD simulation of the SIA diffusion in Be [19, 20] by the density-functional (DFT) code VASP. They found $E_m = 0.12$ eV for the preferential basal plane (BP) diffusion and twice as much, $E_m = 0.27$ eV, for the diffusion out of BP [20]. For $T = 77$ K, this yields $D_I(0.12\text{ eV}) \approx 8.4\cdot10^{-8}$ cm^2/s while $D_I(0.27\text{ eV})\to0$. For a reasonable mean $E_m = 0.2$ eV, $D_I \approx 4.8\cdot10^{-14}$ cm^2/s.

According to Eq. (2), the saturation of $C_I(t)$ occurs at a diffusion-to-sink time $\tau = (k^2\cdot D_I)^{-1}$ which varies from $\sim 10^{-4}$ s for $E_m = 0.12$ eV up to $\sim 10^2$ s for $E_m = 0.2$ eV. In our case, $K_0 \sim 10^{-9}$ s^{-1}, the saturated maximal values of $C_I(\tau) = K_0\cdot\tau$ are $\sim 10^{-13}$ and $\sim 10^{-7}$, respectively. Therefore, $C_I << C_V$ for $t_0 >> \tau$, the V–I recombination rate becomes negligible for $t > t_0$, and the SIA diffusion independent asymptotic (3.2) is fairly applicable.

We applied it to estimate the ELIAS EB exposure time $t_0 = C_V^2 / K_0^2 t^*$ required to inject the requested C_V, say, 10^{-3}. Having $t^* \approx 10^4$ s, we obtained $t_0 \sim 10^8$ s which is more than 3 years long, and is inadmissible.

This issue impels a revision of the models and data used above in this section. There is no vagueness about the values of μ_R, R_d, r_c, and D_0 the more so as the result is D_I independent. Only the dislocation sink strength k^2 remains open to questions. The model (4) neglects the dislocation elastic field which can enhance the SIA capture rate. It also disregards the hcp lattice inherent anisotropy. We suggested the k^2 evaluation (4) looks underestimated, and proceeded to its refined MSMS calculation by means of the MD and kMC simulations.

5. MULTISCALE CALCULATIONS OF THE DISLOCATION SINK STRENGTH

5.1. MD EVALUATION OF THE SIA-EDGE DISLOCATION ELASTIC INTERACTION FIELD

We started from the linear theory of elasticity derived [21] potential energy $U_d(r,\theta)$ of a SIA first-order size interaction with an edge dislocation of Burgers vector **b**$(b,0,0)$. In a cylindrical (r,θ,z) frame of reference with the dislocation line **L** aligned axis z,

$$U_d(r,\theta) = -U_0 b \frac{\sin\theta}{r}, \qquad (6)$$

where the interaction strength factor U_0 has the form

$$U_0 = \frac{\mu}{3\pi}\cdot\frac{1+\nu}{1-\nu}\cdot\delta V, \qquad (7)$$

μ is the elastic shear modulus; ν is Poisson's ratio; δV is the dilative volume change of an isotropic elastic medium due to the presence of a SIA. Hereinafter we neglect the presence of screw dislocations since, for them, U_d is vanished to a first-order of magnitude [21].

The *ab initio* simulations [19, 20] have shown that the basal-octahedral (BO) interstitial position is highly preferential for Be SIAs at low temperatures. Thus, a simple estimate of the SIA dilatation volume difference is $\delta V = \frac{4}{3}\pi\left(R_{Be}^3 - R_{BO}^3\right)$, where $R_{Be} = a/2 \approx 1.14$ Å is the maximal radius of the hexagonally closely packed hard spheres representing Be atoms, $R_{BO} \approx 0.41\cdot R_{Be} \approx 0.47$ Å is the corresponding inner radius of the BO spherical void. This yields $\delta V \approx 5.82$ Å$^3 = 0.72\cdot\Omega_{Be}$ for the reference atomic volume of beryllium $\Omega_{Be} = 8.08$ Å^3.

Substituting this value of δV into (7) together with the up-to-date measured data [22] on the elastic constants of beryllium, $\mu = 150.1$ GPa and $\nu = 0.050$, we obtained the interaction energy factor $U_0 = 0.64$ eV. Other (μ,ν) data taken from the compendium [22] result in the rather close values of $U_0 = 0.58\ldots0.66$ eV. However, notably smaller $U_0 \le 0.5$ eV can be also derived from the earlier measured (μ,ν) reference data [10, 11]. In order to refine the proposed heuristic hard-sphere model, we proceeded to the atomic-scale MD simulation.

The general formula $\delta V = \mathrm{tr}(P_{ij})/3B$ [21] expresses the SIA dilatation volume change in terms of the trace of the point defect dipole-force elastic tensor P_{ij} and the bulk modulus B of an anisotropic medium. We applied the MD code LAMMPS [16] and the Be–Be interatomic potential taken from ref. [23] to calculate P_{ij} according to the following method [24] and algorithm.

To evaluate P_{ij} atomistically, one has to calculate the tensor σ_{ij} of internal stress produced by a solitary point defect in an equilibrated fixed volume V crystallite with periodic boundary conditions (p.b.c.). Then $P_{ij} = -\sigma_{ij}\cdot V$.

The rectilinear p.b.c. $N_1\times N_2\times N_3$ size 3D simulation box of $N = 4\cdot N_1\cdot N_2\cdot N_3$ hcp-Be atoms is first MD equilibrated, by energy minimization at zero temperature, to find its ground state structure, size, and volume V. After that, and with these parameters fixed, the extra Be SIA is inserted into the BP BO position, and the system is MD re-relaxed to its minimal energy at a fixed V. Finally, σ_{ij} is calculated by the LAMMPS code intrinsic routine, and the dipole tensor P_{ij} is found as $-\sigma_{ij}\cdot V$.

To avoid unphysical effects of the crystallite size limitation, this procedure was repeated for the simulation box expanded from 2×2×3 up to 12×12×19 hcp lattice units. It was found that the σ_{ij} components become the box size independent for sufficiently large $N > 10^3$.

For the representative 10944 atoms 12×12×19 box, the BO SIA dipole-force tensor P_{ij} has a diagonal form with principal components $P_{xx} = 2.33$ eV, $P_{yy} = 6.98$ eV, $P_{zz} = 3.24$ eV, and $\mathrm{tr}(P_{ij}) = 13.25$ eV. Using the consistently measured [22] elastic constants $B = 116.8$ GPa, $\mu = 150.1$ GPa, $\nu = 0.05$ of Be, we readily obtained $\delta V = \mathrm{tr}(P_{ij})/3B = 5.73$ Å$^3 = 0.709\cdot\Omega_{Be}$ and, from Eq. (7), $U_0 = 0.63$ eV. This agrees well with the hard-sphere model estimate, 0.64 eV, and thus is quite reliable.

5.2. THE SINK STRENGTH kMC CALCULATION

We treated the diffusion-timescale evolution of point defects statistically as their random walks (RW), mutual annihilations, and absorptions by sinks. The object kMC (okMC) method [25, 26] was applied as the following problem-specific algorithm for the Sandia SPPARKS kMC package [17] to sample all these events.

Vacancies are randomly placed into the hcp Be lattice sites with probability C_{FP}. According to the *ab initio* results [19, 20], only the most energy profitable BO interstitial sites, the centers of the basal plane octahedral voids, are randomly filled by the same number of SIAs. Edge dislocations with Burgers vector $\mathbf{b} = \frac{1}{3}[\bar{2}110]$ are modeled as the $r_c = 2a$ core radius cylinders centered in the $\lambda\times\lambda\times 10\lambda$, $\lambda = \rho_d^{-1/2}$, p.b.c. simulation box.

For the thermally activated diffusion kMC modeling, the frequency Γ_{ij} of a defect transition from i^{th} to j^{th} positions $\mathbf{r}_{i,j}$ is assumed to follow the Arrhenius rule

$$\Gamma_{ij} = \nu_0 \cdot \exp[-E_a(\mathbf{r}_i \to \mathbf{r}_j)/k_B T], \qquad (8)$$

where ν_0 is the transition attempt frequency, E_a is the transition activation energy

$$E_a(\mathbf{r}_i \to \mathbf{r}_j) = E_m(\mathbf{r}_i \to \mathbf{r}_j) + U_d(\mathbf{r}_j) - U_d(\mathbf{r}_i), \qquad (9)$$

E_m is the dislocation elastic field $U_d(\mathbf{r})$ (6) independent migration barrier energy ([20], see in sec. 4).

The reactions events are governed by the following rules. The recombination occurs if the V–SIA distance $\delta r \le r_{eff} = 2a$; both are excluded from simulation. The dislocation trap occurs if the freely migrating SIA is found inside the core, $\delta r_d \le r_c$; then, it is immobilized.

The sketches of this algorithm outputs are shown in Fig. 5 for the same RW step #50. Three **L**-directions, $\{0001\}$, $\{0\bar{1}11\}$ and $\{1\bar{1}10\}$, relevant to Be major slip systems were modeled. Cause of the *ab initio* predicted bias in SIA E_m, 0.12 eV in BP *vs.* 0.27 eV out of it, the major feature of the diffusion anisotropy is clearly seen. SIAs are readily trapped onto the $\{0001\}$ and $\{0\bar{1}11\}$ oriented dislocations while no absorption occurs for the BP parallel $\{1\bar{1}10\}$ sink. The reason is the BP confined SIA diffusion which effectively happens in 2D.

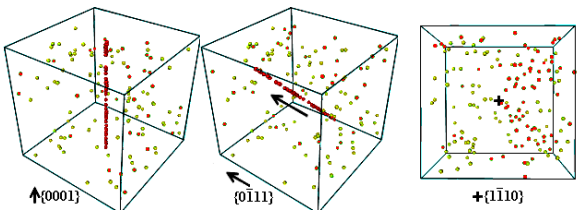

Fig. 5. SPPARKS kMC simulation of Be SIA (●) diffusion, recombination with vacancies (○), and trapping by differently directed edge dislocation sinks, T = 77 K

This okMC algorithm is easily extendable to sinks of other kind and dimensionality (voids, grain boundaries, *etc.*). In general, it can model the solutions of the rate theory ODE system (2) explicitly by the incorporation of the FP source $K(t)$ [25, 26] and at the expense of significant computational efforts. But for the specific semi-analytical framework of our study we shall use it only for calculations of the sink strength k^2.

In Eq. (2.2), $k^2 D_I = 1/\tau$ is the characteristic frequency of SIA absorption by a dislocation sink. Thus, by definition, $k^2 = (D_I \tau)^{-1}$ is a scalar (not a tensor) quantity.

The okMC tally of k^2 within the scope of the d-dimensional RW in $\Re^d$ has been proposed in ref. [25]: $k^2 = 2d/(l^2 \cdot n)$ where l is the $\mathbf{r}_i \to \mathbf{r}_j$ jump length, n is the mean number of jumps each SIA performs before being trapped by a sink (such that $\tau = n/\nu_0$). For the isotropic RW (*e.g.*, in bcc-Fe [26]), $l = l(a)$ is a unique lattice unit dependent constant. Case of hcp-Be, $l_\parallel \ne l_\perp$ (the subscripts $\parallel$ and $\perp$ denote intra- and inter-BP jumps, respectively) and the RW is generally characterized by the (unknown) anisotropic diffusion coefficient tensor $D_{\alpha\beta}$. This implies the $k^2_{\alpha\beta}$ tensor which is out of the scope of the rate theory ansatz (2). To score the properly averaged k^2 as a scalar okMC tally, one has to apply, to it, a certain appropriate probabilistic measure $p(l)$.

The hcp-Be SIA BP-BO lattice has $N_\parallel = 6$ intra-BP closest-neighbor and $N_\perp = 14$ next-neighbor inter-BP BO sites. Following the refined okMC approach [26], we assume the attempt frequency ν_0 to be isotropic, and measure the intra/inter-BP jumps with the probabilities $p_{\parallel,\perp} = N_{\parallel,\perp}\cdot\Gamma_{\parallel,\perp}/(N_\parallel\cdot\Gamma_\parallel + N_\perp\cdot\Gamma_\perp)$, $\Gamma_{\parallel,\perp} = \nu_0\cdot\exp(-E_{\parallel,\perp}/k_B T)$, where $E_{\parallel,\perp}$ are the anisotropic jumps activation energies ($E_\perp >> E_\parallel$ for Be [20]). The averaging operator of this measure is $\langle x\rangle = p_\parallel\cdot x_\parallel + p_\perp\cdot x_\perp$. Let's define the Eq. (2) consistent sink strength as $k^2 = (D_{eff}\cdot\tau_{eff})^{-1}$ with the effective diffusion coefficient $D_{eff} = \langle l^2\rangle/(2d\cdot\langle\delta t\rangle)$ of the isotropic RW jumps of mean square (m.s.) length $\langle l^2\rangle$ and duration $\langle\delta t\rangle$. The effective mean diffusion-to-sink time $\tau_{eff} = n_\parallel\cdot\delta t_\parallel + n_\perp\cdot\delta t_\perp$ is composed from the numbers $n_{\parallel,\perp}$ and durations $\delta t_{\parallel,\perp}$ of intra/inter-BP jumps, $n_\parallel + n_\perp = n$. Since $n_{\parallel,\perp} = p_{\parallel,\perp}\cdot n$, $\tau_{eff} = n\cdot(p_\parallel\cdot\delta t_\parallel + p_\perp\cdot\delta t_\perp) = n\cdot\langle\delta t\rangle$ and, consequently, $k^2 = (D_{eff}\cdot\tau_{eff})^{-1} = 2d/(\langle l^2\rangle\cdot n)$. Therefore, the 'isotropic' k^2 tally [25] is still applicable to score the anisotropic case sink strength, but at a redefined temperature dependent m.s. jump length $\langle l^2\rangle$.

Having $a = 2.286$ Å, $c = 3.584$ Å, $c/a = 1.568$, we obtain $l_\parallel = a = 2.286$ Å, $l_\perp = [(c/2)^2 + (6/7\cdot a)^2]^{1/2} = 2.773$ Å. In a very high temperature limit $k_B T >> E_{\parallel,\perp}$, $\Gamma_{\parallel,\perp} \to \nu_0$, the r.m.s. $l = \langle l^2\rangle^{1/2} \to l_{max} = (9/10\cdot a^2 + 7/40\cdot c^2)^{1/2} = 2.636$ Å. This is an our study irrelevant limiting case of a 3D isotropic SIA diffusion. At low temperatures, $p_\perp << p_\parallel$ and $l \to l_{min} = a = 2.286$ Å also independently on ν_0 and T. This corresponds to an entirely 2D BP SIA diffusion. Calculations show the 3D diffusion RW component sharply appearing just at room temperature, $T \approx 293$ K, and gradually increasing at elevated temperatures.

We applied the developed okMC algorithm to calculate k^2 by means of the SPPARKS kMC code and omitted vacancies as irrelevant to the SIA k^2 evaluation to speed-up the k^2 tally convergence. The per-dislocation normalized dimensionless sink efficiency $\xi = k^2/\rho_d$ kMC calculation results are presented in Figs. 6 and 7.

To uncover the sink strength qualitative regularities, the kMC simulations of Figs. 6, 7 were performed for the $\mathbf{b} = \frac{1}{3}[\bar{2}110]$, **L** = $\{0001\}$ dislocation of Be in wide ranges of temperature T (*incl.* the topical $T = 77$ K), dislocation density $\rho_d = 10^{10}\ldots10^{12}$ cm^{-2} and the dislocation elastic field strength parameter $U_0 = 0.0\ldots0$ eV (*incl.* the quite realistic value

$U_0 = 0.5$ eV). We compared the results with the simplistic T and U_0 independent estimates (4) labeled, in Figs. 6, 7, as the 'isotropic theory'.

One can see that the SIA diffusion anisotropy itself ($U_0 = 0$) has only a small (≤ 50%) temperature independent effect on the SIA trapping efficiency ξ. In contrast to this, the SIA-dislocation interaction affects its absorption very considerably, and results in a drastically (by 1...2 orders of magnitude) increasing ξ. This enhancement is mainly a low-temperature effect, see Fig. 6. It is the most pronounced at $k_B T << U_0$ while tends to disappear at high $k_B T \sim U_0$ when the SIA-to-sink drift is competing with its thermally enhanced chaotic diffusion.

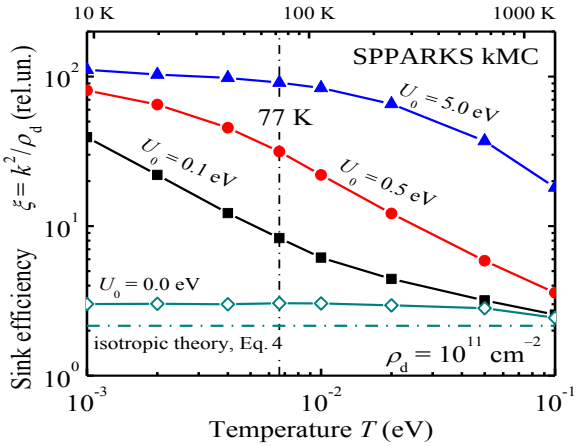

Fig. 6. Temperature dependencies of the normalized efficiency k^2/ρ_d of the {0001} edge dislocation sink at different SIA-dislocation interaction parameters U_0

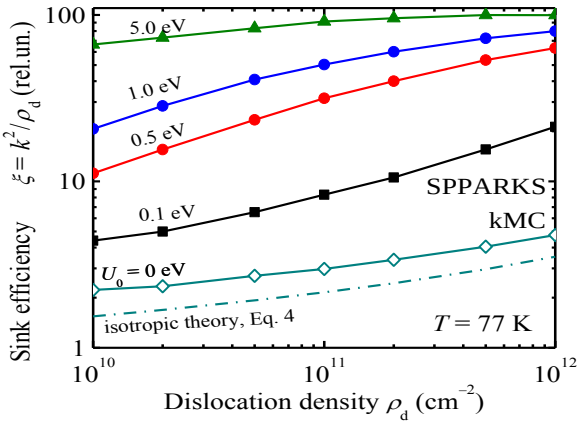

Fig. 7. Dislocation density dependence of the SIA-{0001} sink efficiency for different values of U_0

Fig. 7 clearly shows that the per-dislocation sink efficiency increases with ρ_d. Abt. twofold gain of $\xi(\rho_d)$, at $\rho_d \subset 10^{10\to12}$ cm^{-2}, is predicted already by a field-free isotropic theory (4). For $U_0 = 0.5$ eV and $T = 77$ K, it optimally amounts to ≈ 5. One can see that the kMC calculations confirm both of the proposed features which enhance the SIA sink efficiency, the cryogenic temperature and the highest possible ρ_d of an irradiated sample.

The very significant $\xi(\rho_d)$ anisotropy is found in the Fig. 8 data calculated for three dislocation line directions at the sec. 5.1 MD modeling evaluated $U_0 = 0.63$ eV.

The {0001} dislocations capture SIAs most efficiently. The $\{0\bar{1}11\}$ system is ≈ (25…50)% less efficient, *esp.* at higher ρ_d. The difference is mainly due to the θ-dependence of U_d (6) and, thus, is of the hcp lattice geometry nature. The BP parallel $\{1\bar{1}10\}$ dislocations do not capture SIAs at all ($\xi(\rho_d) \cong 0$ at a SIA low-T 2D diffusion, see in Fig. 5). With respect to our main goal, the mobile SIA removal maximization, this system is lost. Properly textured targets with lowered content of the BP parallel dislocation are favorable. But for the subsequent final calculations, we adopted the cautious hypothesis of an equipartitioning of these slip systems in a Be target.

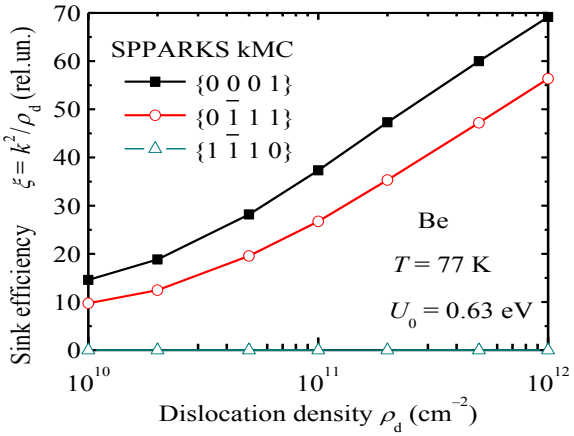

Fig. 8. Anisotropy of the SIA-dislocation sink efficiency

6. RESULTS AND DISCUSSION

The consolidated results of the MSMS calculations of the residual concentrations C_V of surviving vacancies are shown in figures below. They were calculated, according to the rate theory Eqs. (2)–(3), using the Be target parameters (μ_R, k^2, *etc.*) evaluated in sections 4 and 5.

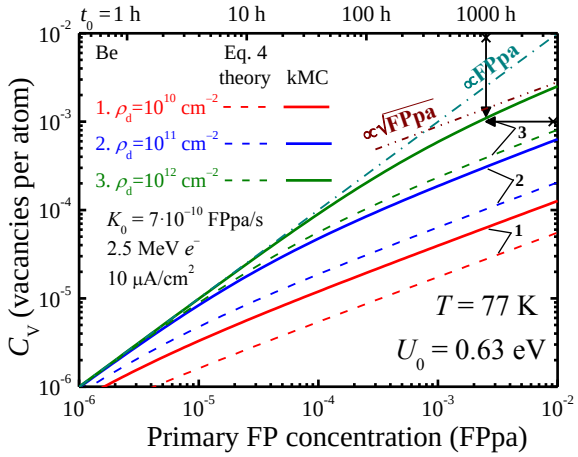

Fig. 9. The residual vacancy concentrations plotted vs. the initial FPpa produced at a EB exposure t_0 (top axis) in Be targets of various dislocation densities ρ_d

In Fig. 9, it is seen that the increase of ρ_d allows to prolongate effectively, in exposure time t_0, the ballistic PRD stage (3.1) (when $C_V \propto$ FPpa) and to delay the occurrence of the kinetic V–I recombination dominance stage (3.2), $C_V \propto (\text{FPpa})^{1/2}$, to much greater t_0. Note that this prediction relies entirely on the results of the adequate MD and kMC calculation of k^2 (sec. 5) since the isotropic field-free theory (4) results in the much more pessimistic data plotted with dashed curves of Fig. 9.

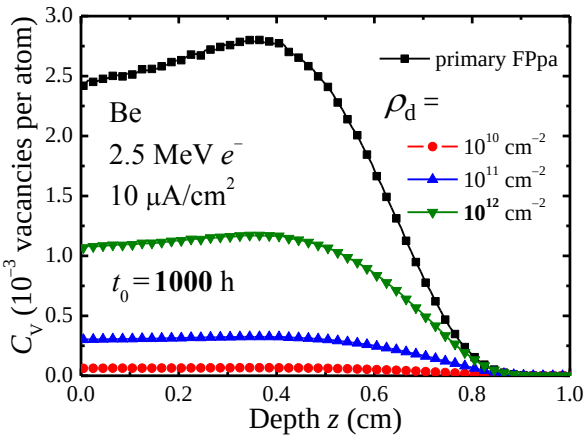

Fig. 10. Depth profiles of the residual C_V in Be targets of different dislocation densities ρ_d (◆,▲,▼) in comparison with the initial FPpa depth profile (■)

Fig. 9 can be used as a diagram for the evaluation of the ELIAS linac EB exposure duration $t_0(C_V)$ needed to obtain the required C_V. The top-right corner arrows indicate this paper topical $t_0(10^{-3}) \approx 10^3$ h for the highest considered $\rho_d = 10^{12}$ cm^{-2}. The depth profiles $C_V(z, t_0)$ were calculated by combining the Fig. 9 data with the primary FPpa rate depth profile $K_0(z)$ of Fig. 4 (sec. 3). In Fig. 10, they are shown for the 1000 h long exposure.

One can see that the most essential is the strong dislocation density ρ_d impact on the residual C_V. In a hypothetical SIA-sink-free beryllium ($k^2 = 0$), the maximal $C_V = (K_0/\mu_R D_I)^{½}$ (see Eq. (2.1)) of the irradiation induced vacancies drops to zero within a FP recombination time $(\mu_R D_I)^{-1} < 10^{-4}$ s just after switching off the EB. In a well annealed beryllium, $\rho_d \sim 10^8$ cm^{-2}, the residual C_V is of $\sim (10^{-6} \ldots 10^{-5})$ even at $t_0 = 10^3$ h. However, Be targets prestrained to $\rho_d \sim 10^{11} \ldots 10^{12}$ cm^{-2} can retain $10^{-4} \ldots 10^{-3}$ vacancies per atom that is sufficient for subsequent cryogenic measurements of their impact on the electronic properties of beryllium. Sinks of all other kinds will promote the SIA outflow enhancing the V–I imbalance in favor of vacancies. Therefore, this work model gives only a lower estimate of the residual C_V, and thus is a conservative evaluation. The estimated EB exposure, 1000 h ≈ 42 days, is rather challenging but is not so impossible bearing in mind the already gained experience of long-time (500…700 h) e^--irradiation of materials at the NSC KIPT operating electron accelerators.

CONCLUSIONS

In the present work, the developed multiscale computer modeling technique was successfully applied to the characterization and planning of cryogenic irradiations at the NSC KIPT sited electron accelerator ELIAS in order to study experimentally the impact of point defects on the superconductivity of beryllium.

The primary radiation damage rate in a target was calculated using the e^--beam transport Monte-Carlo modeling code. The quantitative distinction of the results of its explicit atomistic simulation from the NRT standard model predictions and the considerable contribution of atomic collision cascades into the spatial distributions of primarily produced Frenkel pairs have been revealed.

The later stages of the primary damage time evolution were modeled by different simulation methods basing on the *ab initio* calculated and other reference data on the structure and migration of point defects in Be.

Molecular dynamics modeling has been applied to evaluate the parameters of the elastic interaction of Be self-interstitial atoms with dislocations sinks. Reliable estimates of the dipole-force tensor P_{ij} and the interaction energy factor $U_0 = 0.63$ eV have been obtained.

Kinetic Monte-Carlo modeling has been used for calculation of the dislocation sink strength k^2 basing on *ab initio* and MD data with due account of the hcp-Be anisotropy and the elastic strain of dislocations. The significant growth of k^2 with a decrease in temperature and an increase in the dislocations density has been found. The k^2 anisotropy has been revealed and explained by the preferentially two-dimensional basal plane confined diffusion of self-interstitial atoms at low temperatures.

The concluding data on the multiscale calculated efficiency of the introduction of vacancies into the e^--irradiated Be target were obtained within the scope of the mean-field reaction rate theory. It has been shown that the application of cryogenic (77 K) e^--irradiation of Be targets prestrained up to ~ 10^{12} cm^{-2} dislocation density results in the abnormally high (~ 10^{-3} per atom) yield of residual vacancies which is comparable, to within a half, with that of primarily produced Frenkel pairs at a reasonable (≤ 10^3 h) ELIAS linac e^--beam exposure.

In conclusion, it should be noted that the presented MSMS technique and software are flexible enough to be applied, in future, for the computational support of the other NSC KIPT sited accelerators driven irradiations, including the RMS 'simulation irradiations' with ion beam machines and neutron sources.

ACKNOWLEDGMENTS

The authors are very grateful to A.S. Bakai for drawing their attention to the problem, putting forward the basic idea of future experiments, and for the continuous support and critical discussion of this study. We acknowledge K.V. Kovtun and V.N. Borisenko for valuable data on the prestrained Be targets preparation and the ELIAS linac irradiation e^--beam parameters, opportunities and limitations. We thank I.I. Papirov and A.A. Nikolayenko for provision of their expertise on structural and mechanical properties of beryllium. We also always keep in memory the outstanding role of Yu.T. Petrusenko in providing cryogenic irradiations in NSC KIPT.

REFERENCES

1. ASTM E521-96. *Standard practice for neutron radiation damage simulation by charged-particle irradiation.* Annual Book of ASTM Standards, v. 12.02. American Society for Testing and Materials, Philadelphia, PA, USA, 1996, p. 141-160.

2. M.J. Norgett, M.T. Robinson, I.M. Torrens. A proposed method of calculating displacement dose rates // *Nucl. Eng. Design.* 1975, v. 33, N 1, p. 50-54.

3. M.I. Bratchenko, V.V. Bryk, S.V. Dyuldya, A.S. Kalchenko, N.P. Lazarev, V.N. Voyevodin. Comments on DPA calculation methods for ion beam driven simulation irradiations // *PAST. Ser. "Rad. Dam. Phys. Rad. Mat. Sci."* 2013, N 2(84), p. 11-16.

4. R.E. Stoller. *Primary radiation damage*

formation / R. Konings (ed.). Comprehensive Nuclear Materials. Amsterdam: Elsevier, 2012, v. 1, p. 293-330.

5. G.S. Was. *Fundamentals of radiation materials science: metals and alloys.* Berlin, Heidelberg: Springer-Verlag, 2007, 827 p.

6. J.A. Elliott. Novel approaches to multiscale modelling in materials science // *Int. Materials Reviews.* 2011, v. 56, N 4, p. 207-225.

7. S.I. Golubov, A.V. Barashev, R.E. Stoller. *Radiation damage theory* / R. Konings (ed.). Comprehensive Nuclear Materials. Amsterdam: Elsevier, 2012, v. 1, p. 357-391.

8. S.V. Dyuldya, M.I. Bratchenko. Multiscale modeling of radiation damage in the computational support of accelerator driven simulation studies *// Proc. of the 3rd Int. Conf. "High-purity materials: production, application, properties".* Kharkov: NSC KIPT, 2015, p. 60.

9. S.V. Dyuldya, M.I. Bratchenko. Methodology and software for multiscale modeling of radiation impact on materials *// Abstr. of XV Conf. "HEP. Nucl. Phys. Accelerators."* Kharkov: NSC KIPT, 2017, p. 51-52.

10. I. Papirov, A. Nikolayenko, Yu. Tuzov. *Beryllium:* monograph. M.: MEPhi NNRU, 2017, 344 p.

11. I.I. Papirov. *Handbook on the structure and properties of beryllium alloys.* M.: "Energoatomizdat", 1981, 368 p.

12. A.S. Bakai, A.N. Timoshevskii, S.A. Kalkuta, A. Moeslang, V.P. Vladimirov. On the influence of vacancies on the electronic properties of beryllium // *Low Temp. Phys.* 2007, v. 33, issue 10, p. 889-891.

13. A. McKinley (Jr.), H. Feshbach. The Coulomb scattering of relativistic electrons by nuclei *// Phys. Rev.* 1948, v. 74, N 12, p. 1759-1763.

14. A.S. Bakai, M.I. Bratchenko, S.V. Dyuldya. Impact of the highly deformed Be dislocation structure on the point defects kinetics at the NSC KIPT ELIAS linac cryogenic electron irradiation *// Abstr. of the XIII Conf. "HEP. Nucl. Phys. Accelerators".* Kharkov: NSC KIPT, 2015, p. 85.

15. S.V. Dyuldya, M.I. Bratchenko. Refined model and code for calculation of point defects concentrations in multicomponent heterogeneous materials *// Proc. of the ICPRP-XX,* Alushta, Sept. 10–15, 2012. Kharkov: NSC KIPT, 2012, p. 42-43.

16. S. Plimpton. Fast parallel algorithms for short-range molecular dynamics // *J. Comput. Phys.* 1995, v. 117, N 1, p. 1-19; http://lammps.sandia.gov.

17. S. Plimpton, C. Battaile, M. Chandross, et al. *Crossing the mesoscale No-Man's Land via parallel Kinetic Monte Carlo.* SANDIA Report SAND2009-6226, Oct. 2009; http://spparks.sandia.gov.

18. F.A. Nichols. On the estimation of sink-absorption terms in reaction-rate-theory analysis of radiation damage // *JNM.* 1978, v. 75, issue 1, p. 32-41.

19. M.G. Ganchenkova, P.V. Vladimirov, V.A. Borodin. Vacancies, interstitials and gas atoms in beryllium: ab initio study // *JNM.* 2009, v. 386-388, N 1, p. 79-81.

20. V.A. Borodin, P.V. Vladimirov. Self-interstitial diffusion in beryllium: elementary jumps and overall dynamics *// Proc. of the 10th IEA Int. Workshop on Beryllium Technology,* Sept. 19–21, 2012, Karlsruhe, Germany. KIT Sci. Publ., 2012, p. 318-326.

21. C. Teodosiu. *Elastic models of crystal defects.* Berlin Heidelberg: Springer-Verlag, 1982, 336 p.

22. A. Migliori, H. Ledbetter, D.J. Thoma, T.W. Darling. Beryllium's monocrystal and polycrystal elastic constants // *J. Appl. Phys.* 2004, v. 95, N 5, p. 2436-2440.

23. C. Björkas, K.O.E. Henriksson, M. Probst, K. Nordlund. A Be–W interatomic potential // *J. Phys.: Cond. Matter*. 2010, v. 22, N 35, 352206 (6 p.).

24. E. Clouet, S. Garruchet, H. Nguyen, M. Perez, C.S. Becquart. Dislocation interaction with C in α-Fe: A comparison between atomic simulations and elasticity theory // *Acta Materialia*. 2008, v. 56, N 14, p. 3450-3460.

25. L. Malerba, C.S. Becquart, Ch. Domain. Object kinetic Monte-Carlo study of sink strengths // *JNM.* 2007, v. 360, N 2, p. 159-169.

26. A.B. Sivak, V.M. Chernov, V.A. Romanov, P.A. Sivak. Kinetic Monte-Carlo simulation of self-point defect diffusion in dislocation elastic fields in bcc iron and vanadium // *JNM*. 2011, v. 417, N 1-3, p. 1067-1070.

Article received 02.11.2017

МНОГОУРОВНЕВОЕ МОДЕЛИРОВАНИЕ ЭЛЕКТРОННОГО ОБЛУЧЕНИЯ БЕРИЛЛИЯ ПРИ НИЗКИХ ТЕМПЕРАТУРАХ

М.И. Братченко, С.В. Дюльдя

Представлены методология и результаты многомасштабного моделирования первичной генерации и временной эволюции радиационных дефектов при криогенном (77 К) облучении сильнодеформированного до плотности дислокаций ~ 10^{12} см$^{-2}$ бериллия на электронном линаке ELIAS ННЦ ХФТИ. Показано, что применение низкотемпературного облучения предварительно напряженных мишеней позволяет эффективно подавлять рекомбинацию пар Френкеля за счет ухода свободно мигрирующих собственных межузельных атомов на дислокационные стоки и приводит к аномально высоким (~ 10^{-3} на атом) выходам вакансий, сопоставимых с концентрациями первичных пар Френкеля при разумной (≤ 10^3 ч) длительности e^--облучения.

БАГАТОРІВНЕВЕ МОДЕЛЮВАННЯ ЕЛЕКТРОННОГО ОПРОМІНЕННЯ БЕРИЛІЮ ЗА НИЗЬКИХ ТЕМПЕРАТУР

М.І. Братченко, С.В. Дюльдя

Представлено методологію та результати багатомасштабного моделювання первинної продукції та еволюції у часі радіаційних дефектів за криогенного (77 К) опромінення сильнодеформованого до густини дислокацій ~10^{12} $см^{-2}$ берилію на електронному лінаці ELIAS ННЦ ХФТІ. Показано, що застосування низькотемпературного електронного опромінення попередньо напружених мішеней дозволяє ефективно пригнічувати рекомбінацію пар Френкеля через витік вільно мігруючих власних міжвузельних атомів до дислокаційних стоків і призводить до аномально високих (~10^{-3} на атом) концентрацій вакансій, які добре порівнянні з концентраціями первинних пар Френкеля за прийнятної (≤ 10^3 год) тривалості електронного опромінення.